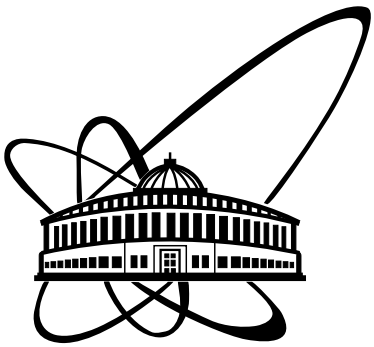

Nucleation Theory and Applications

Jürn W. P. Schmelzer, Gerd Röpke, and Vyatcheslav B. Priezzhev (Editors)

Dubna JINR 2006

6 Solid State of Repelling Particles

Boris M. Smirnov[(1)] *and R. Stephen Berry*[(2)]

[(1)] *Institute for High Temperatures, Izhorskaya 13-19, Moscow 127412, Russia*

[(2)] *Department of Chemistry, University of Chicago, 5735 South Ellis Avenue, Chicago, IL 60637, USA*

Better be wise by the misfortunes of others than by your own.

Aesop

Abstract

The peculiarity of an ensemble of repelling particles at low temperatures, where interaction between nearest neighbors dominates its properties, is its polycrystalline structure with a density of particles lower than that of the crystal lattice. This result follows from computer simulations, model experiments with filling a container with hard balls, and the virial theorem. Moreover a polycrystalline structure is observed directly in a colloid solution. The question arises of whether such a polycrystalline state of an ensemble of repulsed atoms at low temperatures is thermodynamically stable, or is a metastable, glassy state that results from the kinetics of relaxation of this ensemble to low temperatures and high densities. The disk model for repelling particles and the cell model for the configurations of these particles show that the glassy state of this system under indicated conditions is thermodynamically favorable.

6.1 Introduction

We consider ensembles of particles with a sharply varying repulsive potential between them, and suppose that these ensembles are supported by external pressure

or other external forces. Table 6.1 gives examples of such particle ensembles; we include in this list a dusty plasma with Yukawa interaction potentials between particles for a screening length of this interaction potential less than the mean distance between nearest particles. All the above systems are simple and, like systems of bound atoms, have two aggregate states, solid and liquid, as follows from computer simulations and observations [1, 2, 3, 4].

One can expect that the liquid state of these systems corresponds to a random spatial distribution of particles, but in the solid, the particles form a face-centered cubic (fcc) or hexagonal structure, in which each internal particle has 12 nearest neighbors. But in reality an ensemble of repelling particles in the solid state has a polycrystal structure, i.e. a long-range order is not realized for such particle ensembles. This follows from model experiments with filling a container with hard balls [4, 5, 6, 7], from computer simulations within the framework of hard sphere model [4, 8, 9, 10], and from the virial theorem for the crystal state of an ensemble of repelling atoms under an external pressure [11]. Moreover, the polycrystalline structure of a colloid solution was observed directly by light scattering [13]. Thus, repelling atoms do not form an infinite crystal lattice.

Tab. 6.1 Ensembles of repelling particles and boundary conditions that allow one to concentrate the particles in a restricted spatial region

Ensemble of particles	Boundary conditions
Inert gases under high pressure	External pressure
Hard balls in a box	Pressure due to weight of upper particles
Colloid solutions	External pressure
Dusty plasma	Electric traps

The crystal structure of repelling atoms at high pressure and low temperatures is unstable thermodynamically according to the virial theorem [11, 12]. But the virial theorem deals with uniform particle distributions, and this prohibition relates to an infinite crystal rather than to the domain structure of an ensemble of repelling atoms when this ensemble includes individual crystallites. This distribution in colloid solutions is considered as a glassy state [14, 15, 16, 17] because of the long times for equilibrium establishment when the density of monomer particles is high. This means that the kinetics of relaxation processes to low temperatures and high densities does not allow a system to reach a state close to the crystal, under these conditions. We also show, with a simple model, that the

kinetics of particle displacements involves obstacles along the way to establishing a favorable particle distribution in a space within the framework of simple model. Specifically, we introduce a disk model for a system of repelling particles, and the cell model for their spatial distribution when this distribution is close to that in crystals.

6.2 Ensembles of Repelling Particles at Low Temperatures

We consider ensembles of identical classical particles with a pair interaction between them, so that the pair interaction potential $U(r)$ at a distance r between particles can be approximated by

$$U(r) = U(R_o)\left(\frac{R_o}{r}\right)^k = \frac{A}{r^k}\,, \tag{6.1}$$

Moreover, we take this interaction potential to vary sharply at a critical distance, i.e.

$$k = \frac{d\ln U}{d\ln r} \gg 1\,, \tag{6.2}$$

so a test particle interacts only with nearest neighbors. In this limit one can use the model of hard spheres for interaction of particles, so that the pair interaction potential can be changed to the following one [18]

$$U(r) = \begin{cases} \infty\,, & \text{for} \quad r \le 2a\,, \\ 0\,, & \text{for} \quad r > 2a\,, \end{cases} \tag{6.3}$$

where a is the effective particle radius.

In spite of identical interactions between particles for different ensembles of repelling particles of Table 6.1, these ensembles due to different external conditions all exhibit a particular behavior at low temperatures where they have a polycrystalline structure. An individual crystallite probably contains less than hundreds of balls in the case of a container filled with hard balls [5, 6, 7]. A typical size of an individual crystallite of inert gas under high pressure is estimated to be $\sim 10^3$ [11, 12]. In the case of colloid solutions, an individual crystallite contains $\sim 10^6 - 10^7$ monomers [13]. In a dusty plasma the particles form a unit crystal

in the solid state [19], but the absence of the polycrystalline structure in this case may be explained by a restricted number of particles that does not exceed $10^4 - 10^5$. This difference can be explained by the weakness of the processes which provide the formation and existence of a group of particles-monomers with crystal structure, and therefore these processes depend on external conditions. In particular, gravity is of importance for colloidal crystals [20].

Nevertheless, the tendency to reach the polycrystalline structure is identical for the various ensembles of repelling particles which are given in Table 6.1. This tendency and the character of formation of the polycrystalline structure can be described by the hard sphere model for particle interactions. This allows one to study the character of evolution of ensembles of repelling particles using the hard sphere model with standard molecular dynamics [21]. Hence we will use the results of molecular dynamics based on the hard sphere model for various properties of particle ensembles under consideration.

If the hard sphere model is applicable for particle interactions, it is convenient to characterize the distribution of the hard spheres in space by the packing parameter [4], given by

$$\varphi = \frac{4\pi}{3n} r^3 N \ , \tag{6.4}$$

where r is the sphere's radius, N is the number density of spherical particles, n is the number of particles inside a given sphere, and the packing parameter φ is the fraction of the space occupied by hard particles. Evidently, the maximum value of this parameter for hard spheres corresponds to a close-packed crystal lattice for which the packing parameter is

$$\varphi_{cr} = \frac{\pi\sqrt{2}}{6} = 0.74 \ . \tag{6.5}$$

The packing parameter φ of an ensemble of hard spheres follows from simple experiments based on filling a container with hard balls [5, 6, 7] and on simulations with hard spheres [8, 9, 10]. The observed value $\varphi_d = 0.64$ [6] is in accord with a more precise value from computer simulations for the packing density of this system [9]

$$\varphi_d = 0.644 \pm 0.005 \ . \tag{6.6}$$

This means that an ensemble of hard spheres does not form an infinite close-packed crystal lattice. Using the connection of the mean coordination number q

(an average number of nearest neighbors for a test particle) with the corresponding atom density ρ [22], we find

$$q = 12\frac{\rho}{\rho_{cr}} , \tag{6.7}$$

where ρ_{cr} is the crystal density. With $q = 12$ for the close packed structure, we have, on the basis of Eqs. (6.4) and (6.5), for an average number of nearest neighbors at the maximum packing parameter Eq. (6.6)

$$q = 12\frac{\varphi}{\varphi_{cr}} = 16.2\varphi , \tag{6.8}$$

Eqs. (6.5) and (6.7) give $q = 10.4 \pm 0.1$, close to the coordination number of liquid inert gases at low pressures, in which atoms are bonded by attractive forces, and for which $q = 10.1 \pm 0.1$ [22, 23].

Note that although the ensemble of repelling particles does not form an infinite crystal lattice, it exhibits short-range order. In particular, the correlation function Q_6 [24], that is zero for an amorphous structure, is not zero for an ensemble of hard spheres [9]. Therefore this ensemble is separated into individual crystallites.

Meanwhile, the time of establishment of an equilibrium spatial distribution of particles in such a system increases sharply with an increase of the packing parameter from $\varphi_m = 0.545$ for the solid state at the melting point up to its maximum value φ_d. For example, a typical time to establish an equilibrium distribution in colloids in experiment [20] varies from 1 hour up to several days, with the packing parameter varying from φ_m up to $\varphi = 0.62$.

Thus, in spite of the simplicity, the structure of solid systems of repelling particles is not as simple as one might expect at a first sight, and an ensemble of repelling particles includes clusters, i.e. crystallites. Hexagonal structure of these crystallites is preferred for colloid solutions, although they may also contain an admixture of the fcc structure [20, 25, 26]. For compressed inert gases, only the hexagonal structure is observed in the limit of high pressures [27]. The surface of an individual crystallite is nonspherical and is similar to that of a fractal aggregate. The fractal dimension for the crystallite in the colloid case is 2.35 ± 0.15 [26].

6.3 Model of Hard Disks for an Ensemble of Repelling Atoms

In order to understand the properties of a classical ensemble of strongly repelling particles and the character of its relaxation as a result of displacements, it is convenient to use the model of hard disks, the simplest model for such an ensemble of particles locked in a box. We consider a two-dimensional case to simplify the problem of repelling particles; this allows us to extract the principal properties of the ensemble in a simple manner. To characterize the particle density in a box, we introduce the packing parameter like that of Eq. (6.4), for the three-dimensional case

$$\varphi = \frac{\pi a^2 n}{S} \,, \tag{6.9}$$

where a is the radius of a particle-disk, n is the number of particles inside the box, and S is the area of a square inside the box. Evidently, the maximum of the packing parameter corresponds to the crystal lattice of the hexagonal structure that provides the most packing of particles. Then the distance between neighboring particles of the same line is $2a$, and the distance between neighboring lines of particles is $a\sqrt{3}$, i.e. the density of a bulk crystal of the hexagonal structure is $(2a^2\sqrt{3})^{-1}$. Correspondingly, the packing parameter for the bulk hexagonal crystal

$$\varphi_{hex} = \frac{\pi}{2\sqrt{3}} = 0.907 \tag{6.10}$$

is the maximum of the packing parameter that is possible for particle-disks.

We will operate with an element of this lattice that contains 16 particles. This element may be cut out of the crystal lattice. We place it in a rhombic box (Fig. 6.1) where these particles are packed densely. Then the angles between rhombus sides are $\pi/3$ and $2\pi/3$, and the side length is $(6 + 4/\sqrt{3})a = 8.309a$. The packing parameter for this system is less than that for a bulk hexagonal lattice and is equal to

$$\varphi_{16} = \frac{8\pi\sqrt{3}}{(3\sqrt{3}+2)^2} = 0.841 \,. \tag{6.11}$$

One can construct ensembles of particles in a box with one vacancy (Fig. 6.2) and two vacancies (Fig. 6.3), by removal of one and two atoms from an element

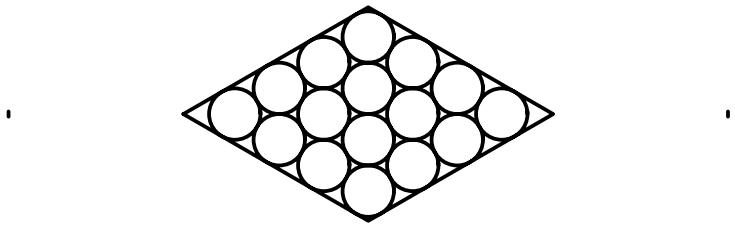

Fig. 6.1 An element of the hexagonal structure consisting of 16 particle-disks in a box

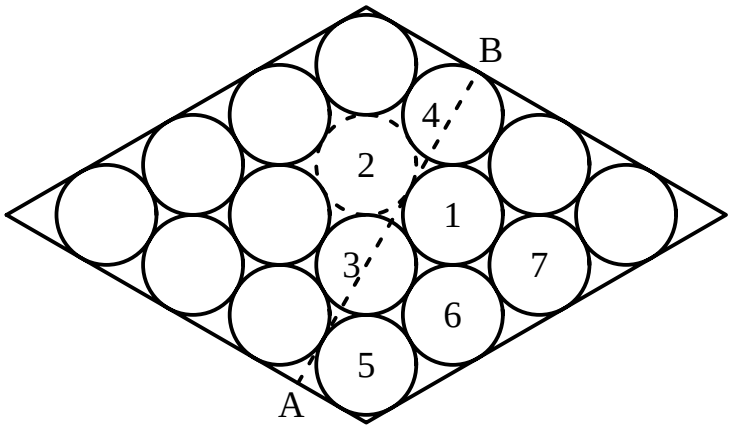

Fig. 6.2 An element of the hexagonal structure of Fig. 6.1 in a box with one vacancy

of Fig. 6.1. The packing parameters for these ensembles in these cases are given by

$$\varphi_{15} = \frac{15}{16}\varphi_{16} = 0.788\ , \qquad \varphi_{14} = \frac{14}{16}\varphi_{16} = 0.736\ . \tag{6.12}$$

In the latter case two vacancies may be transformed into two voids, as shown in Fig. 6.4 for a symmetric configuration of the particles and voids. In contrast to vacancies, voids can change their shape and size in the course of evolution.

But the dense packing of Fig. 6.2 does not allow for particles and vacancy to change their positions. Indeed, a particle 1 of Fig. 6.2 can transfer to the position

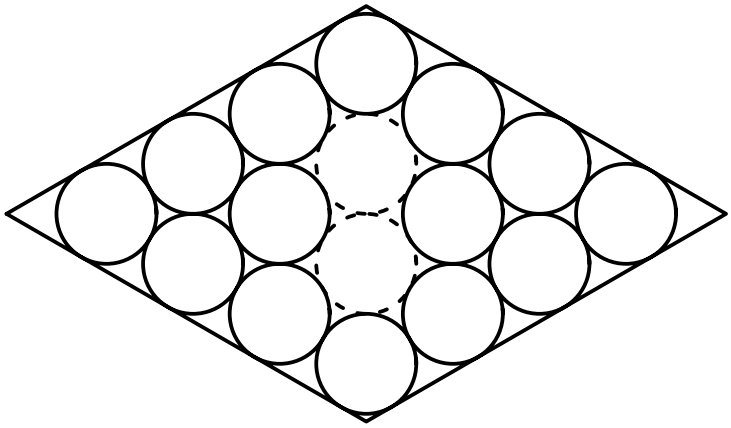

Fig. 6.3 An element of the hexagonal structure of Fig. 6.1 in a box with two vacancies

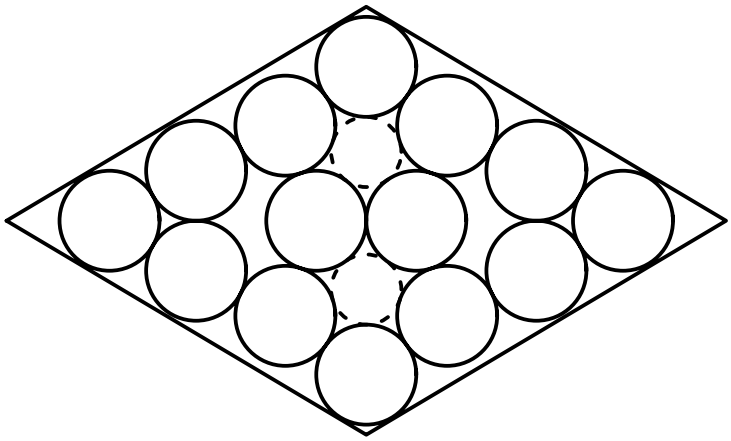

Fig. 6.4 An element of the hexagonal structure of Fig. 6.1 in a box with two voids

2 if the distance between two neighboring particles 3 and 4 exceeds $4a$, whereas it is $2a + a\sqrt{3}$ for close packing of the particles. This particle transition becomes possible, if we increase the box size.

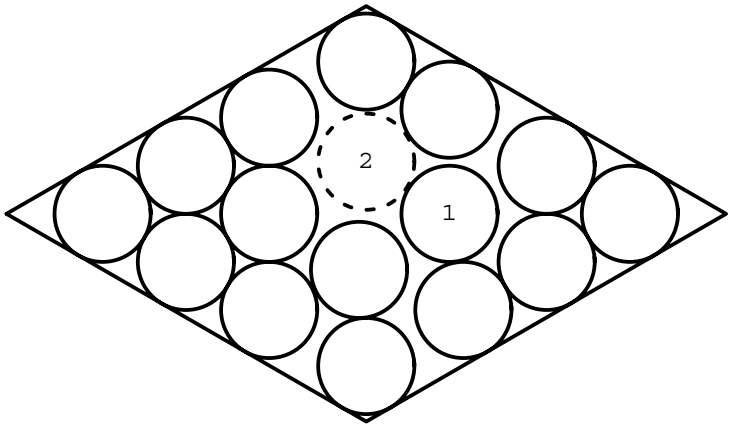

Fig. 6.5 Particle-disks in a box at the density that ensures transitions of particles and voids to other positions

Let us introduce the parameter r, so that a rhombus side for the box is

$$l = \left(6 + \frac{4}{\sqrt{3}}\right) r \ . \tag{6.13}$$

Under conditions of Fig. 6.1 we have $r = a$, and we consider below the case $\Delta r = r - a \ll a$ when relative positions of particles-disks in a box change slightly. The distance AB of Fig. 6.2 is equal to $(3\sqrt{3}+2)a$ and becomes $(3\sqrt{3}+2)r$ after a boxwidening. For passing of a particle 1 into a new position it is necessary to increase the initial value AB at least by $(2-\sqrt{3})a$, i.e. this value exceeds $(4+2\sqrt{3})a$. Thus, a particle 1 of Fig. 6.2 may transfer to a position 2, if the criterion $r - a \geq 0.037a$ is fulfilled, as takes place under conditions of Fig. 6.5, if

$$(3\sqrt{3}+2)r \geq (4+2\sqrt{3})a \tag{6.14}$$

or $r \geq 1.037a$. This corresponds to the packing parameter

$$\varphi \geq \left(\frac{a}{r}\right)^2 \varphi_{15} = 0.732 \ . \tag{6.15}$$

This value is approximately that of the packing parameter for formation of two vacancies as given in Fig. 6.3. Note that the critical packing parameter for particle transition depends on the box shape.

In the same manner one can find the minimum packing parameter required for a particle transition between positions 6 and 1 of Fig. 6.2. On the basis of the above consideration, we obtain Eq. (6.15) for the packing parameter in this case. Next, let us consider a transition between positions 5 and 6 of Fig. 6.2 or between positions 5 and 3, when one of these positions is located in a box angle and, of course, one of transition positions is free. This transition is possible if the length AB is increased by $(2-\sqrt{3})a$, which allows transfer of an angle particle or of another particle to an angle position. We obtain the minimal packing parameter for particle transfer in this case also in accordance with Eq. 6.7.

Thus, we find the critical value of the packing parameter when transitions of particles and vacancies are possible in a box under the conditions given above. This consideration is based on conservation of the particle configuration in the course of box widening, i.e. it requires that the criterion $\Delta r = r - a \ll a$ holds true. This criterion gives $\Delta r \geq 0.037a$; this requirement may be fulfilled. At the critical value of the packing parameter, the diffusion coefficient for particles in a box due to their thermal motion is zero; it increases with a decrease of the packing parameter. For s small number of particles the diffusion coefficient in a box depends also on a box shape.

6.4 Equation of State for Disks

A disk model for particles confined in a finite space is a simplified description of an ensemble of repelling particles. First, this simplification uses a two-dimensional space that allows us to study geometric properties of the ensemble in an obvious manner. Second, assuming within the framework of this model, that particles interact only during their contact, we reduce the problem of a condensed-phase system to that of a dense gas, since a time of particle contact is brief in comparison with the time between two subsequent contacts of these particles with one another. Therefore, though the mean free path of particles may be small compared to their size, particles move freely most of the time. Thus, the behavior of particles in a condensed system within the framework of the disk model is rather like that in a gaseous system. Below we derive the equation of state for a bulk ensemble of such particles.

Characterizing the particle density in a box by the packing parameter φ, we assume the particle's spatial distribution to be random, i.e. $\varphi < \varphi_{hex}$, although these values have the same order of magnitude. Fig. 6.6 gives the trajectory of the center of a test particle located near the plane boundary-wall and encounters

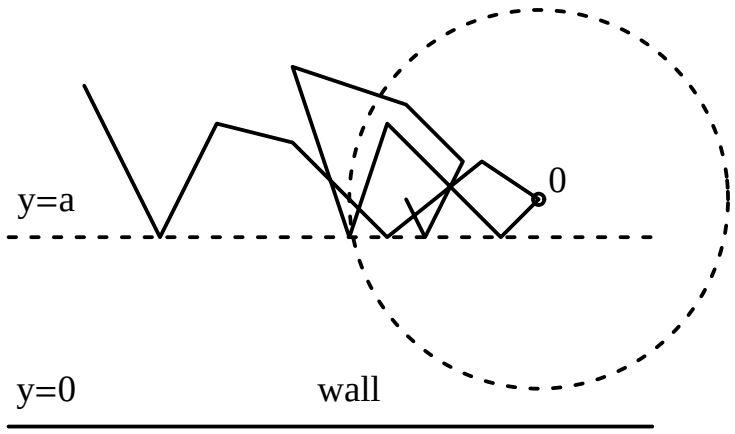

Fig. 6.6 Trajectory of the center of a surface particle. The particle-disk with center O is shown by a dashed circle

it. The particle center of course cannot approach to the wall closer than its radius a. This particle reflects elastically from the wall at each contact. Then it collides with surrounding particles and returns to the wall.

Let us estimate the force on the wall due to collisions of a test surface particle. Assuming a Maxwell distribution of particle velocities, we have for a typical particle momentum $P \sim (mT)^{1/2}$, where m is the particle mass, T is the temperature expressed in energetic units. Since collisions of a test particle with the wall occur in a mean time $\tau \sim \lambda/v_T$, where λ is the mean free path and v_T is a typical particle velocity ($v_T \sim (T/m)^{1/2}$, one can use this to estimate the mean force transmitted to the wall by a test particle at the surface

$$F \sim \frac{T}{\lambda} \,. \tag{6.16}$$

From this expression, one can derive the equation of state for an ensemble of particles by introducing the pressure p as the force per unit area that acts on the walls.

Let us consider first the gaseous case in which the particle number density N is small, and particles that reach the walls are located in a layer of a width $\sim \lambda$.

Therefore the number of particles per unit area of the surface is $\sim N\lambda$, and the equation of state takes the form $p \sim NT$. More specifically, it has the form

$$p = NT \; . \tag{6.17}$$

In the case under consideration, in which we deal with a dense ensemble of particles, we obtain for $\varphi \sim 1$ and $N \sim a^{-3}$, instead of Eq. (6.17),

$$p = cNT\frac{a}{\lambda} \; , \tag{6.18}$$

where the numerical coefficient $c \sim 1$. Thus, applying the gaseous criterion leads to another equation of state for a dense ensemble of particles [28, 29, 30]. In the case of a high density of disks, it is convenient to introduce a small parameter

$$\alpha = \frac{S - S_o}{S_o} \; , \tag{6.19}$$

where S is the area per individual particle-disk, and S_o is its limit for the close-packed structure. Then the equation of state for this ensemble of particles-disks can be given in the form

$$p = NTF(\alpha) \tag{6.20}$$

and the function $F(\alpha)$ is given by [30]

$$F(\alpha) = \frac{2}{\alpha} + 1.90 + 0.67\alpha + 0(\alpha^2) \; . \tag{6.21}$$

6.5 The Cell Model for Disk Particles

We consider now the cell model of particles [8, 31, 32] in which the particles can be located in certain cells. In particular, within the framework of the disk model, these cells may be circles as shown in Fig. 6.7.

Let us determine the partition function for this system at a specified value of the packing parameter. Starting from the hexagonal structure of disks with the packing parameter $\varphi_{hex} = 0.907$, we decrease the packing parameter. Within the framework of the cell model this can proceed in two (nonexclusive) ways, either by an increase of the radius r of an individual cell that exceeds the disk radius a, or by formation of vacancies. Let the initial area contain $n + v$ cells, of which

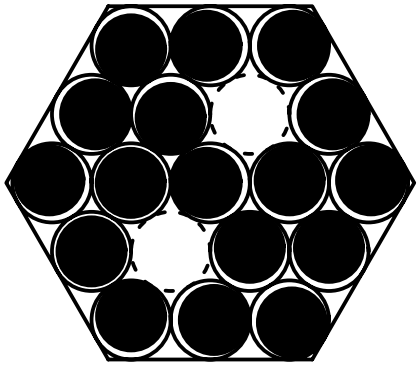

Fig. 6.7 The cell model, in which disk particles (solid circles) are located in their cells (open circles)

n are occupied by particles (i.e. v empty cells are vacancies). Then the packing parameter is

$$\varphi = \varphi_{hex} \frac{n}{n+v} \left(\frac{a}{r}\right)^2 \ . \tag{6.22}$$

The partition function of this system with an accuracy up to a constant factor is equal to

$$Z = C_{n+v}^n \left(\frac{r^2 - a^2}{a^2}\right)^n \ . \tag{6.23}$$

We take the partition function of an individual particle in its cell to be proportional to the area $\pi(r^2 - a^2)$ that can be occupied by this particle in its cell; the first factor of this formula takes into account permutations of particles and cells.

In order to obtain a thermodynamically stable state, it is necessary to optimize the entropy $S = \ln Z$ with respect to the number of vacancies at a given value of the packing parameter φ. For large values of n and v we have

$$\begin{aligned} S = \ln Z &= \ln C_{n+v}^n + n \ln \left(\frac{r^2 - a^2}{a^2}\right) \\ &= n \ln \left(1 + \frac{v}{n}\right) + v \ln \left(1 + \frac{n}{v}\right) + n \ln \left(\frac{r^2 - a^2}{a^2}\right) \ . \end{aligned} \tag{6.24}$$

Expressing the cell radius from Eq. (6.22) and substituting it into Eq. (6.25), we find for the entropy per particle ($s = S/n$) the result

$$s = c \ln \left(1 + \frac{1}{c} \right) + \ln(c_{max} - c) \; , \tag{6.25}$$

where the vacancy concentration is introduced as $c = v/n$, and its maximum value at a given packing parameter φ is attained when the cell radius is equal to the particle radius ($r = a$). This is

$$c_{max} = \left(\frac{\varphi_{hex} - \varphi}{\varphi} \right) \; . \tag{6.26}$$

To deduce Eq. (6.25), we take the cell radius r at a given packing parameter φ from Eq. (6.14) and substitute it into Eq. (6.15). Note that the entropy per particle s is defined with accuracy up to a constant.

For optimization of cell and particle distributions we find the vacancy concentration c_o that corresponds to the maximum entropy. If $\varphi \sim \varphi_{hex}$, this corresponds to a low value of the optimal vacancy concentration given approximately by

$$c_o = \exp \left(- \frac{1 + c_{max}}{c_{max}} \right) \; . \tag{6.27}$$

This value varies from 0.012 up to 0.12, if c_{max} varies from 0.2 up to 0.6, corresponding to a variation of the packing parameter from 0.76 to 0.57. Thus, within the framework of the disk model for particles, a decrease of the packing parameter leads mostly to an increase of the cell radius, while only a small part of the increase of area per particle goes into formation of new vacancies.

Note that an ensemble of disk particles can be considered as a gas because the interactions between particles are assumed to occur only when they touch each other, making the interaction time of a test particle with a neighbor brief compared with the time when this particle is free. Evidently, in a real condensed system of repelling particles, a test particle interacts with nearest neighbors strongly, i.e. at each time the interaction potential energy of a test particle with surrounding particles is comparable to its kinetic energy.

In order to understand the role of interactions between particles in establishing their optimal space distribution, we analyze below the contribution of these interparticle interactions to the entropy of the entire ensemble. The entropy for the cell model when particles are found in cell centers, on average, has the form

$$S = \ln Z = \ln C_{n+v}^{n} + n \ln \left(\frac{r^2 - a^2}{a^2} \right) - qn \frac{U(r)}{T} \, , \tag{6.28}$$

where $q = 6 - c$ is the average number of nearest neighbors of a test particle, $U(r)$ is the pair interaction potential at a distance r between particles, and we change the interaction potential between nearest particles to that at the average interparticle distance. The temperature T is expressed in energetic units. This gives the entropy variation

$$ds = dc \left[\ln(1 + \frac{1}{c}) - \frac{1 - c_{max}}{(1 + c)(c_{max} - c)} + \frac{U(r)}{T} - \frac{qk}{2} \frac{U(r)}{T} \frac{1}{1 + c} \right] \, . \tag{6.29}$$

From this formula it follows that including terms proportional to $U(r)/T$ decrease the entropy as the cell radius decreases. Hence the optimal conditions correspond to a lower vacancy concentration c than that for the hard disk model.

6.6 Diffusion Coefficient of Vacancies for Cell Model

We now estimate the diffusion coefficient of particles or vacancies in a dense ensemble of disk-particles within the framework of the cell model. Transitions of particles between cells are shown in Fig. 6.8; these lead to reverse transitions of vacancies. Hence the diffusion coefficients of particles D_p and vacancies D_v are connected by a simple relationship

$$D_p = cD_v \, , \tag{6.30}$$

because they result from the same process.

We first estimate a typical time of particle transition to a neighboring cell (see Fig. 6.9). For simplicity, we place a transferring particle-disk in the center of its cell. The transitions are possible with small angles with respect to the arrow of Fig. 6.9 if a transferring disk does not touch its neighbors in the course of the transition. If a test particle is moving along the arrow and a neighboring particle

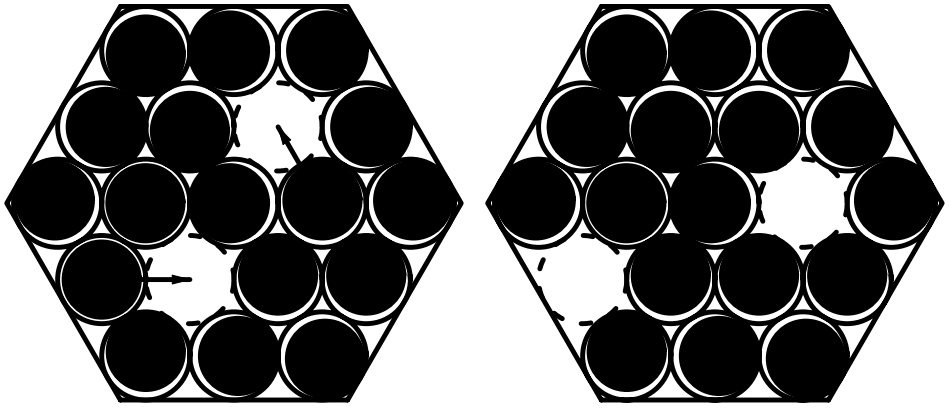

Fig. 6.8 Transition of particle-disks to neighboring positions within the framework of the cell model. The initial configuration of particles is left and the final configuration is given right; the arrows indicate the transferring particles

occupies a favorable position in its cell being touching the cell circle, the gap between particles is equal to

$$\Delta = (1 + \sqrt{3})r - 3a \ , \tag{6.31}$$

From this relation, on the basis of the condition $\Delta > 0$, we have the packing density of particle-disks when the diffusion coefficient for particles or vacancies is nonzero, and displacement of vacancies and particles is possible in the interior of the particle ensemble

$$\varphi < \varphi_{hex} \left(\frac{1 + \sqrt{3}}{3} \right)^2 = 0.75 \ . \tag{6.32}$$

The diffusion process for particles inside their ensemble ceases at values above this packing parameter.

To estimate the vacancy diffusion coefficient, we recognize that a transferring particle collides elastically many times with its nearest neighbors as a result of its thermal motion, and that this goes on until the angle between its velocity direction and an arrow like that of Fig. 6.9 would be below θ, so that

$$\theta \sim \frac{\Delta}{r} \ . \tag{6.33}$$

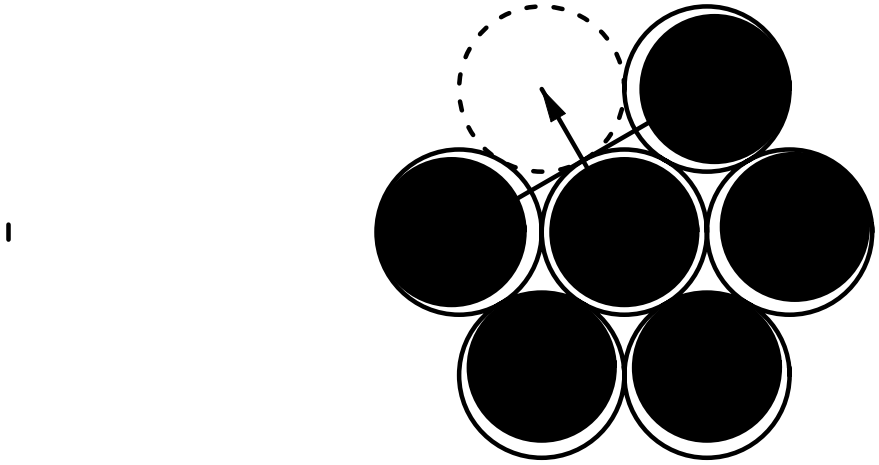

Fig. 6.9 Transition of a particle-disk to a neighboring cell through a line separating neighboring cells. The transition proceeds along an arrow or at small angles to it

Correspondingly, a typical transition time of a test particle to a free neighboring cell is

$$\tau \sim \frac{r-a}{v_t}\theta \sim \frac{(r-a)\Delta}{v_T r} \,. \tag{6.34}$$

We consider a range of the packing parameter values when $R \sim a$ and $r - a \ll a$. Note that $r - a \approx 0.1a$ at $\Delta = 0$. From this we obtain an estimate of the vacancy diffusion coefficient in a dense ensemble of particle-disks as

$$D_v \sim \frac{r^2}{\tau} \sim \frac{a\Delta v_T}{r-a} \,. \tag{6.35}$$

Hence the vacancy diffusion coefficient $D_v \to 0$ if $\Delta \to 0$.

We again take into account that the disk model for an ensemble of repelling particles models this ensemble as a gas of particles and therefore cannot describe some properties of this system. In particular, this model gives a general character of particle diffusion inside this system, but does not automatically reveal the temperature dependence of this quantity. We now estimate this dependence within the framework of the cell model.

The diffusion process has an activation character, and the temperature dependence for the diffusion coefficient has the form

$$D_v \sim \exp\left(-\frac{E_a}{T}\right) , \tag{6.36}$$

where E_a is the activation energy, and T is the temperature expressed in energy units.

Let us locate particles in the centers of their cells and determine the activation energy of the diffusion process for this particle configuration. Then the activation energy is the difference of the interaction potentials for a transferring particle located midway between the initial and final positions and in its initial (or final) position. Accounting for interactions with nearest neighbors in those initial, midway and final positions of a transferring particle, we obtain in this case

$$\begin{aligned} E_a = {} & 2U\left(\frac{r\sqrt{3}}{2}\right) + 4U\left(\frac{r\sqrt{7}}{2}\right) + 2U\left(\frac{3r}{2}\right) \\ & - 5U(r) - 2U\left(r\sqrt{30}\right) - U(2r) . \end{aligned} \tag{6.37}$$

In particular, approximating the pair interaction potential of particles by the dependence $U(r) \sim r^{-k}$ and taking $k = 8$, we obtain

$$E_a = 0.36U_o , \tag{6.38}$$

where $U_o = 5U(r)$. Accounting for displacements of particles inside their cells would decrease the barrier energy.

As follows from this formula, within the framework of the hard disk model, the diffusion coefficient of vacancies becomes zero for values of the packing parameter Eq. (6.32) because a high particle density does not allow a particle to transfer to a neighboring free cell. Repulsive interactions between particles can reinforce this effect at low temperatures, and then diffusion of vacancies and particles cease at even lower densities.

6.7 Peculiarities of the Solid State of an Ensemble of Repulsing Particles

Simple models considered here confirm once more that repelling particles do not form a crystal lattice in the solid state. The polycrystalline atomic structure may be considered as a glassy state as it is done for colloid solutions [14, 15, 16, 17]. One might think that this is not a major issue, but in reality it is important.

Indeed, the uniform crystal structure is not thermodynamically stable according to the virial theorem [11] alone, but a polycrystalline state does not submit to the virial theorem and of course it can be realized. But since this state is not a unique, thermodynamically stable form, different values of the parameters of this structure are possible. In particular, the number of monomers, i.e. particles not nested in crystalline structures, in a typical assembly of microcrystalline clusters depends both on the physical object and on its method of preparation, including the rate at which it makes its transition into its final state. As with other glassy systems, one can expect that a typical size of a crystalline cluster in the system will be larger, the slower is the process of preparation of the solid state. Evidently, this explains (or at least rationalizes) the different sizes of individual crystalline particles for different objects, as discussed in the introduction to the present chapter.

In particular, let us consider the solid state of inert gases at low temperatures and high pressures. Such a state can be prepared by two methods. One can fix the temperature and increase the pressure, starting from the crystal structure at the triple-point pressure, or one can start from the liquid state at high pressure and decrease the temperature at a constant pressure. In the first case the stacking instability that corresponds to displacement of layers, will lead to transition from an fcc lattice to the hexagonal structure for atoms of nearest layers. Since the displacement of layers becomes difficult after layers in other directions are displaced, this method can lead to a higher density of atoms than that from the second method, in which we start from an amorphous atomic distribution, and creation of small crystallites results from diffusion of vacancies and voids to the outside of the system. In the same manner, one can conclude that the final density for the second method depends on the rate of cooling since the final density is determined by diffusion of atoms and voids.

Thus, we conclude that the glassy nature of the solid state of an ensemble of repelling atoms can lead to different internal parameters of these objects depending on their nature and preparation method. Nevertheless, all these objects have

polycrystalline structure, although the sizes of individual crystallites can depend both on the substance and the method of its production.

6.8 Conclusion

This analysis of an ensemble of repelling classical particles on the basis of simplest models exhibits the nature of the structure and diffusion of this particle ensemble. The domain structure established by a temperature decrease or a density increase may become frozen at some particle density because displacement of particles becomes impossible. Therefore, these solid states of the particle-disk ensemble have features of a glassy state.

Acknowledgments

R.S.B. would like to acknowledge support from the National Science Foundation. B.M.S. thanks the Russian Foundation for Basic Research (Grant 03-02-16059) for partial support.

6.9 References

1. B. J. Alder and T. E. Wainwright, J. Chem. Phys. **27**, 208 (1957).

2. W. G. Hoover, S. G. Gray, and K. W. Johnson, J. Chem. Phys. **55**, 128 (1971).

3. S. M. Stishov, Sov. Phys. Uspekhi **17**, 625 (1974); UFN **114**, 3 (1974).

4. I. Gutzow and J. Schmelzer, *The Vitreous State: Thermodynamics, Structure, Rheology, and Crystallization* (Springer, Berlin, 1995).

5. J. D. Bernal, Nature **183**, 141 (1959).

6. G. D. Scott, Nature **178**, 908 (1960).

7. J. D. Bernal and J. Mason, Nature **188**, 908 (1964).

8. W. G. Hoover and F. H. Ree, J. Chem. Phys. **49**, 3609 (1968).

9. M. D. Rintoul and S. Torquato, Phys. Rev. Lett. **77** 4198 (1996).

10. M. D. Rintoul and S. Torquato, Phys. Rev. **58E**, 533 (1998).

11. R. S. Berry and B. M. Smirnov, Phys. Rev. **71B**, 051510 (2005).

12. R. S. Berry and B. M. Smirnov, Phys. Uspekhi **48**, 331 (2005); UFN, **175**, 367 (2005).

13. P. N. Pusey et al., Phys. Rev. Lett. **63**, 2753 (1989).

14. L. V. Woodcock, J. Chem. Soc. Faraday II **72**, 1667 (1976).

15. W. van Megen and S. M. Underwood, Phys. Rev. Lett. **70**, 2766 (1993); Phys. Rev. **E 49**, 4206 (1994).

16. R. J. Speedy, J. Chem. Phys. **100**, 6684 (1994).

17. J. Yeo, Phys. Rev. **E52**, 853 (1995).

18. B. M. Smirnov, *Physics of Ionized Gases* (Wiley, New York, 2001).

19. V. E. Fortov et al., Phys. Uspekhi **47**, 447 (2004).

20. J. Zhu et al., Nature **387**, 883 (1997).

21. B. J. Alder and T. E. Wainwright, J. Chem. Phys. **33**, 1439 (1960).

22. B. M. Smirnov, Phys. Uspekhi **37**, 1079 (1994).

23. B. M. Smirnov, *Clusters and Small Particles in Gases and Plasmas* (Springer, New York, 2000).

24. P. J. Steinhardt, D. R. Nelson, and M. Ronchetti, Phys.Rev. **B28**, 784 (1983).

25. S. Auer and D. Frenkel, Nature **409**, 1020 (2001).

26. U. Gasser et al., Science **292**, 258 (2001).

27. H. Cynn et al., Phys. Rev. Lett. **86**, 4552 (2001).

28. Z. W. Salsburg and W. W. Wood, J. Chem. Phys. **37**, 798 (1962).

29. W. G. Hoover, J. Chem. Phys. **44**, 221 (1966).

30. B. J. Alder, W. G. Hoover, and D. A. Yang, J. Chem. Phys. **49**, 3688 (1968).

31. J. G. Kirkwood, J. Chem. Phys. **18**, 380 (1950).

32. C. H. Bennet and B. J. Alder, J. Chem. Phys. **54**, 4796 (1971).